

Stability, Transition and Turbulence

M. Y. Hussaini

Institute for Computer Applications in Science and Engineering

NASA Langley Research Center

Hampton, VA 23665

1 Abstract

A glimpse is provided of the research program in stability, transition and turbulence based on numerical simulations. This program includes both the so-called abrupt and the restrained transition processes. Attention is confined to the prototype problems of channel flow and the parallel boundary layer in the former category and the Taylor-Couette flow in the latter category. It covers both incompressible flows and supersonic flows. Some representative results are presented.

2 Nomenclature

C_p	: specific heat at constant pressure
C_v	: specific heat at constant volume
D	: average of diagonal stress components
\mathbf{F}	: forcing function
M	: Mach number
OD	: average of off-diagonal stress components
p	: pressure
Pr	: Prandtl number
Re	: Reynolds number
t	: time
T	: temperature
\mathbf{u}	: fluid velocity
γ	: ratio of specific heats (C_p/C_v)
δ	: Kronecker tensor
∇	: gradient operator
κ	: thermal conductivity
μ	: molecular viscosity
Φ	: viscous dissipation function
ρ	: density
S	: average of stress components on the scalar level
σ	: viscous stress tensor
θ	: $(T - T_w)/(T - T_\infty)$
V	: average of stress components on the vector level

Superscripts

\sim : Favre average

Subscripts

k, l : Cartesian indices

w : wall value

∞ : freestream value

3 Introduction

The phenomena of transition to turbulence are so complex as to defy a unified theory at the present time. As such, direct numerical simulations of these phenomena within the framework of Navier-Stokes equations have assumed a dimension equal in importance to experimental and even theoretical studies. An effective simulation not only mimics a physical experiment but has the added advantages of offering readily retrievable clean information wherever and whenever it is needed, and also a precise control of parameters unachievable in the physical experiment. Theoretical and mathematical approaches provide progress in understanding through the processes of abstraction and idealization; the results of analysis then furnish, apart from specific predictions, a deeper comprehension of the underlying general principles. These features are not intrinsic to a numerical simulation. However, they can be built into the simulations to some extent. Careful considerations of such factors are the bases of the research program in this area. Here at LaRC/ICASE our research program includes both the so-called abrupt and restrained transition processes. Attention is confined to the prototype problems of the channel flow and the parallel boundary layer in the former category, and the wake and the Taylor-Couette flows in the latter category. It covers both incompressible flows and supersonic flows.

4 Poiseuille and Blasius Flows

4.1 Background

Although our knowledge of laminar-turbulent transition is by no means complete, the broad features are now clear at least in low subsonic shear flows. This is in a large measure due to the the classical experiments of Klebanoff, Tidstrom and Sargent [1], Kovaszny, Komoda and Vasudeva [2], Hama and Nutant [3]. These experiments were conducted in a controlled, identifiable disturbance environment where the nondeterministic disturbances were immeasurably small. Briefly stated, the instability and transition process involves the following stages: 1) a primary instability evolving in accordance with the linear theory, 2) a secondary instability leading to the emergence of a flow of a pronounced three-dimensional nature, and the appearance of the streamwise vortex system, 3) the development of detached high-shear layers, 4) at least a tertiary instability (if not an extremely rapid succession of a sequence of instabilities) resulting in turbulent spot development and 5) convection and coalescence of turbulent spots to form a fully developed turbulent flow. Similar patterns have been observed in plane Poiseuille flow by Nishioka, Iida and Ichikawa [4]. More recently, the experiments of Kachanov and Levchenko [5], and Saric and Thomas [6] have uncovered some new details in the secondary instability stage of the transition process in boundary layers. The flow pattern outlined above is relevant to natural transition under some limited, but not all, conditions. The reviews of Stuart [7] and Tani [8] provide a detailed discussion of the classical experiments and the then available theoretical explanations of the isolated stages or events of the transition process. The more recent review of Herbert and Morkovin [9] provides an overview of applied problems in stability and transition, and a discussion of the various theoretical approaches to the secondary instability problem. Craik's monograph [10] deals with the general problem of wave interactions in various fields, and includes a discussion of the secondary instability pertinent to wall-bounded shear flows.

The primary instability has as its basis linear theory and has long been well established. The theory for the secondary instability is however more recent, but is also fairly well established (Herbert [11], Nayfeh [12]). There have been no improvements in the theoretical models for the other stages since the survey article of Stuart [7] Full scale numerical simulations provide a unified basis for investigating the

relevance and relative importance of various events right up to the formation of turbulent spots. In the present paper we shall dwell on numerical experiments which have uncovered the secondary instability associated with the center modes in plane Poiseuille flow. We shall also discuss simulations which have brought out the relative effectiveness of the various laminar flow control (LFC) techniques such as heating, favorable pressure gradient and suction. We will present some representative results in each category.

The incompressible variable property Navier-Stokes equations, in usual notation, are (Zang and Hussaini [13])

$$\nabla \cdot \mathbf{u} = 0 \quad (1)$$

$$\frac{\partial \mathbf{u}}{\partial t} + \mathbf{u} \cdot \nabla \mathbf{u} = -\nabla p + \frac{1}{Re} \nabla \cdot (\mu \nabla \mathbf{u}) + F_{\mathbf{u}} \quad (2)$$

$$\frac{\partial \theta}{\partial t} + \mathbf{u} \cdot \nabla \theta = \frac{1}{RePr} \nabla \cdot (\kappa \nabla \theta) + F_{\theta} \quad (3)$$

where the lengths are scaled by the half channel-width (or for the boundary layer by the displacement thickness at the streamwise station of interest), velocities by the corresponding center velocity for the channel flow (or the corresponding mainstream velocity for the boundary layer), and pressure by the dynamic head; the forcing functions $F_{\mathbf{u}}$ and F_{θ} are designed to ensure parallel flow. The viscosity and conductivity are given functions of temperature for the heated wall case, and constants in other cases.

The applied boundary conditions assume periodicity in the horizontal directions, and the no-slip velocity on solid walls. For the heated water boundary layer case, the no-slip condition for the velocity and a uniform temperature are enforced at the wall; perturbations are assumed to be zero in the mainstream. This permits a Fourier discretization in the streamwise and spanwise directions, and a Chebyshev discretization in the vertical direction. The initial condition consists of a triad of waves - one two-dimensional wave and two skewed waves. The general fractional step algorithm for efficiently solving the relevant equations is given by Zang and Hussaini [14]. A survey of spectral algorithms for fluid dynamic calculations is given in Hussaini and Zang [15], and Canuto, Hussaini, Quarteroni and Zang [16]. The latter is a monograph which deals with both theory and applications of spectral methods.

4.2 Instability Due To A Triad Of Center Modes

The so-called center modes of plane channel flows are in fact temporal eigenfunctions of the Orr-Sommer-

field equation which decay in time. However, a combination of a two-dimensional center mode with two skewed modes is susceptible to an instability similar to the secondary instability encountered in a similar non-resonant triad of wall modes. The essential qualitative difference between the center mode and the wall mode (as is evident from Fig. 1a and 1b) is that the maximum amplitude for the former occurs away from wall towards the channel center, while for the latter it occurs near the wall, and hence the terminology. There are of course other quantitative differences with regard to wavelengths, phase velocities and decay rates. The Reynolds number for the simulation was 8000 based on the channel half width, and both the streamwise and spanwise wavenumbers were unity; the initial two-dimensional and three-dimensional amplitudes were 10% and 3% respectively of the channel center velocity. The resolution requirements were monitored and the grid was refined to resolve the fine structures as they emerged. The finest grid was 96x128x192. Plotted in Fig. 2 is the time history of the harmonic contents of the solution. Note that the two-dimensional mode, labeled (1,0), decays almost exponentially, but the three-dimensional mode, labeled (1,1), grows after an initial decay for about three periods 2π being the characteristic period. The results are presented at $t = 87$ (a little less than 14 periods) at which time the finest grid was just about sufficient to resolve the sharp gradients of the flow field. The vortex lines are displayed in Fig. 3a, and for comparison purposes vortex lines for an analogous case of wall modes are presented in Fig. 3b. The streamwise and spanwise vorticity contours are displayed in Fig. 4 at four equidistant streamwise planes over a wavelength. Fig. 5 displays similar contours for the case of the wall modes. The qualitative similarities and differences are obvious. The center-mode vortex loop is comparatively away from the wall, and the pinching at the neck is less intense than for the wall-mode vortex loop. Also, the high-shear layer associated with the center modes is less intense than the one associated with the wall modes. The physical relevance of the center mode instability to the high-intensity bypass to transition is as yet undetermined.

4.3 Effect of Heating on the Secondary Instability of Blasius Flow

Laminar flow control (LFC) vehicles might operate in a finite-amplitude disturbance environment, so it is of interest to examine the relative performance of the various LFC techniques in the nonlinear regime.

While some experimental studies have investigated the influence of nonlinear disturbance sources such as roughness, vibrations, free-stream turbulence, etc. on the basic transition process, there have been no comparative studies on the sensitivity of the LFC techniques such as heating, pressure gradient and suction in the nonlinear regime. In the absence of any relevant nonlinear stability theories due to the complexity of the problem, numerical simulations can play a crucial role in this field. As an example of such a use of simulation, we have performed a Navier-Stokes calculation involving conditions similar to those used in the experiment of Kovaszny, Komoda and Vasudeva [2] except that in our simulation the wall was heated. The idealization of a parallel boundary layer was used mainly in order to meet the resolution requirements while keeping the computing time within reasonable limits. The Reynolds number of the simulation was 1100 based on the displacement thickness, and the initial amplitudes of the two-dimensional and three-dimensional Tollmien-Schlichting waves (wall modes) were respectively 2.7% and 0.8% of the free stream velocity. The finest grid was 72x162x192.

Three different situations were studied: 1) the uncontrolled case, 2) the heated fixed temperature case, and 3) the heated active temperature case. In the heated fixed temperature case, the temperature was kept fixed at the initial value pertinent to the mean flow conditions, and the temperature evolution was totally neglected. In the heated active temperature case, the temperature evolution was taken into account by solving the temperature equation along with the momentum equations. In both the cases the wall temperature was 2.75% above the free stream temperature. Fig. 6 shows the harmonic history of the perturbation energy. Note that the (1,0) mode which grows in the uncontrolled case decays in the heated almost up to 4 periods. Heating damps the (1,1) mode initially, but it starts growing within the first period. It appears that when the energy in the three-dimensional wave overtakes that in the two-dimensional wave, it feeds energy partly into the two-dimensional wave. Fig. 7 shows the spanwise vorticity contours on the peak plane. In the uncontrolled case (Fig. 7 top left) a kink develops in the high-shear layer at time t equal to three Tollmien-Schlichting periods. It is generally accepted that a irrevocably quick succession of events follows thereafter leading to a turbulent spot formation. Heating the wall to 2.75% above the free stream temperature diffuses the high-shear layer as is obvious from Fig. 7 (bottom left). However, within the subsequent one and one fourth period, turbulent spot formation appears to become imminent (Fig. 7 top right). In the fixed

temperature case, it is clear from Fig. 7 (bottom right) that the high-shear layer formation is mellowed down even up to four and one fourth periods. The fixed temperature case overpredicts the weakening effect of heating on the secondary instability. In other words, the effect of temperature evolution is significant and deleterious in the nonlinear regime whereas it is quite negligible in the linear regime.

5 Taylor-Couette Flow

The instability and abrupt transition process are typical of aerodynamic flows. On the other hand, the transition to turbulence by spectral evolution are typical of geophysical fluid dynamics where there is a destabilizing force field. The Taylor-Couette flow in the annulus of concentric rotating circular cylinders typifies a class of geophysical problems involving instabilities and turbulence due to the presence of a destabilizing centrifugal force field. DiPrima and Swinney [17] provide an excellent review of instabilities and transitions in Taylor-Couette flows. Our interest lies in finite-length Taylor-Couette flow as it offers the situation of weak turbulence which is amenable to direct simulation. The prime objective of our research effort to examine the various qualitative mathematical theories (Benjamin [18]). Some of the routes to mathematical chaos appears to have been observed in these flows. The chaos theories are based on model equations. Our investigations will establish the relevance of these theories to Navier-Stokes equations.

This problem, unlike those considered in the preceding sections, is truly inhomogeneous in two directions. A spectral algorithm necessarily involves Chebyshev polynomial expansions in radial and axial directions, and Fourier expansion in the azimuthal direction. The fractional step algorithm used to study the channel flows and the parallel boundary layers is easily extended to treat this problem (Streett and Hussaini [19]).

The initial phase of study focussed on the steady-state bifurcations in axisymmetric Taylor-Couette flow (with the inner cylinder rotating, and the outer cylinder and end walls remaining stationary) for aspect ratios of order unity. These problems provide a stringent test for a time-accurate method designed to simulate the delicate unsteady processes leading to transition. Among the numerous simulations carried out to compare with the available experiments, we present some typical results for the geometry of Benjamin and Mullin [20] which had an aspect ratio

of 1.05 and radius ratio of 0.615. The symmetric two-cell mode is established at a relatively low Reynolds number of 62, and then the Reynolds number is impulsively raised to 150. The development of the asymmetric single-cell flow represented by the streamlines in a cross-sectional plane is shown in Fig. 8, and Fig. 9 displays the order parameter (which is a measure of the asymmetry of the flow) and energy as functions of time in units of characteristic diffusion time scale. The continuing simulations are on the verge of capturing bifurcations into time-dependent states. The final objective is to calculate the dimension of the strange attractor which is supposed to represent the weak turbulence.

6 Compressible Transition and Turbulence

Transition to turbulence in supersonic and hypersonic flows is a gray area. There are differing experimental results, and unexplained visual observations. The picture is quite piecemeal compared to low Mach number flows. The purpose of the research program is to answer questions such as: a) do secondary instability mechanisms observed in low subsonic flows persist in supersonic flows, b) is the turbulent spot formation the usual way transition occurs, and c) is the transition process abrupt or restrained. The initial focus of our research program is on question (a), i.e., whether the known prototypes of instabilities in incompressible flows persist at high Mach numbers. A spectral simulation of a three-dimensional instability process in a parallel boundary layer at Mach number 4.5 was carried out.

The full compressible Navier-Stokes equations are, in dimensionless form, (Erlebacher and Hussaini [21])

$$\frac{\partial \rho}{\partial t} + \nabla \cdot (\rho \mathbf{u}) = 0 \quad (4)$$

$$\frac{\partial (\rho \mathbf{u})}{\partial t} + \nabla \cdot (\rho \mathbf{u} \mathbf{u}) = \frac{1}{Re} \nabla \cdot \boldsymbol{\sigma} \quad (5)$$

$$\frac{\partial p}{\partial t} + \mathbf{u} \cdot \nabla p + \gamma p \nabla \cdot \mathbf{u} = \frac{\gamma}{Re Pr M_\infty^2} \nabla \cdot (\mu \nabla T) + (\gamma - 1) \Phi \quad (6)$$

where

$$\sigma_{ki} = \left[\mu \left(\frac{\partial u_k}{\partial x_i} + \frac{\partial u_i}{\partial x_k} \right) - \frac{2}{3} \mu (\nabla \cdot \mathbf{u}) \delta_{ki} \right] \quad (7)$$

$$\Phi = \frac{1}{2} \left(\frac{\partial u_k}{\partial x_i} + \frac{\partial u_i}{\partial x_k} \right) \sigma_{ki} \quad (8)$$

and the equation of state is

$$\gamma M_\infty^2 p = \rho T \quad (9)$$

with $\gamma = C_p/C_v$, the ratio of specific heats. At high Mach number, temperature variations across the boundary layer become important and the temperature dependence of viscosity must be taken into account. The Prandtl number was assumed equal to 0.7, and the Sutherland's law was prescribed for viscosity variation with the temperature. The free stream Mach number was 4.5, and the Reynolds number was 10000 based on the displacement thickness. The boundary conditions were identical to those used in the incompressible boundary layer simulations discussed in the earlier section. The initial condition consisted of an unstable two-dimensional wave and a pair of three-dimensional oblique waves superimposed on a prescribed parallel mean flow. These waves were the eigenfunctions of an eighth order eigenvalue problem, the compressible analogue of the incompressible Orr-Sommerfeld equation. The initial amplitudes of the two-dimensional and three-dimensional perturbations were taken to be respectively 5.4% and 1.2% of the free stream velocity. The temporal evolution of this triad of waves was followed for about eight periods of the initial two-dimensional Tollmien-Schlichting wave (TS wave). The time history of several Fourier harmonics of the perturbation kinetic energy (integrated in the vertical direction) is shown in Fig. 10. After a period of slow growth of the three-dimensional wave, labeled (1,1) mode, the nonlinear interactions between the (0,1) spanwise mode and the primary (1,0) mode trigger the secondary instability after approximately 5 TS periods. Contour plots of the streamwise velocity (Fig. 11) at the time of 5 TS periods illustrate the incipient stages of a K-type breakdown (Erlebacher and Hussaini [21]). In the supersonic simulations, the critical layer is an order of magnitude further from the wall than in the incompressible cases. One consequence is that the structures are farther removed from the walls. Initial results indicate that compressibility retards the onset of the secondary instability. However, a more extensive parameter study is required before any firm conclusion can be drawn.

Our research program has recently focused its attention on the development of subgrid-scale models for compressible turbulence. A compressible extension of Bardina's linear combination model [22] has been developed. Favre-averaging was employed to produce spatially averaged compressible Navier-Stokes equations which closely resemble the incompressible ones. For compressible as opposed to incompressible flow, the trace of the subgrid stresses

cannot be incorporated with the pressure since the pressure is a true thermodynamic variable. These isotropic stresses must now be modeled, and a new model constant, termed the isotropic constant, must be included.

This new model has been tested against direct simulations at Mach numbers ranging from 0.0 to 0.6 and on grids of 64^3 to 128^3 . The turbulence model was compared against this direct simulation (DS) data suitably injected onto a coarser grid. The coarse grid would normally be used in a large eddy simulation. A least square fit between the total stress calculated from the DS and the modeled stress computed from spatially filtered velocities allows the constants to be determined. The constant determination was performed on the vector level (Erlebacher, Hussaini, Speziale, Zang [23]). Table 1 summarizes the correlation coefficients between the modeled and the exact

	$M_0 = 0.0$	$M_0 = 0.6$
<i>D</i>	82	81
<i>OD</i>	85	84
<i>V</i>	72	71
<i>S</i>	73	74

Table 1:

total stresses at Mach 0 and Mach 0.6. Results are presented on the tensor, vector and scalar levels. The vector level is the divergence of the tensor, while the scalar level is defined by the product of $\nabla \cdot \tilde{u}$ and \tilde{u} . The Leonard stress is omitted from the total subgrid stress because it can be calculated exactly. Correlation coefficients of over 80% are obtained on the tensor level, and above 70% on both the vector and scalar levels. A more thorough study can be found in Erlebacher et al. [23].

7 Concluding Remarks

Numerical algorithms for studying the physics of transition and turbulence in simple geometries have been developed. Detailed studies of the highly nonlinear stages of transition prior to turbulent spot formation have been made. The use of simulations to study the sensitivity of laminar flow control techniques in the nonlinear regime has been demonstrated. A new instability mechanism associated with the center modes in channel flows has been uncovered, although

its physical significance is as yet undetermined. The first numerical simulations of their kind are being carried out for supersonic boundary layer flows. The preliminary results revealed the existence of a secondary instability similar to the one in incompressible flows.

References

- [1] Klebanoff, P. S.; Tidstrom, K. D.; and Sargent, L. M.: The Three-Dimensional Nature of Boundary-Layer Instability, *J. Fluid Mech.*, Vol. 12, 1962, pp. 1-34.
- [2] Kovasznay, L. S.; Komoda, H.; and Vasudeva, B. R.: Detailed Flow Field in Transition, Proc. 1962 Heat Transfer and Fluid Mechanics Institute, pp. 1-16, Stanford Univ. Press, Palo Alto, 1962.
- [3] Hama, F. R.; and Nutant, J.: Detailed Flow-Field Observations in the Transition Process in a Thick Boundary Layer, Proc. of the 1963 Heat Transfer and Fluid Mechanics Institute, pp. 77-93, Stanford Univ. Press, Palo Alto, 1963.
- [4] Nishioka, M.; Asai, M.; and Iida, S.: An Experimental Investigation of the Secondary Instability in Laminar-Turbulent Transition, *Laminar-Turbulent Transition*, R. Eppler and H. Fasel (eds.), pp. 37-46, Springer-Verlag, Berlin, 1980.
- [5] Kachanov, Yu. S.; and Levchenko, V. Ya.: The resonant interaction of disturbances at laminar-turbulent transition in a boundary layer, *J. Fluid Mech.*, Vol. 138, 1984, pp. 209-247.
- [6] Saric, W. S.; and Thomas, A. S. W.: Experiments on the subharmonic route to turbulence in boundary layers, *Turbulence and Chaotic Phenomena in Fluids*, T. Tatsumu (ed.) North Holland, 1984.
- [7] Stuart, J. T.: Hydrodynamic Stability, *Appl. Mech. Rev.*, Vol. 18, 1965, pp. 523-531.
- [8] Tani, I.: Boundary-Layer Transition, *Ann. Rev. of Fluid Mech.*, Vol. 1, 1969, pp. 169-196.
- [9] Herbert, T.; and Morkovin, M. V.: Dialogue on bridging some gaps in stability and transition research, *Laminar-Turbulent Transition*, R. Eppler and H. Fasel (eds.), pp. 47-70, Springer Verlag, Berlin, 1980.
- [10] Craik, A. D. D.: *Wave Interactions and Fluid Flows*, Cambridge University Press, 1985.
- [11] Herbert, T.: Floquet analysis of secondary instability in shear flows, *Stability of Time Dependent and Spatially Varying Flows*, D. L. Dwoyer and M. Y. Hussaini (eds.), pp. 43-57, Springer Verlag, New York, 1987.
- [12] Nayfeh, A. H.: On secondary instabilities in boundary layers, *Stability of Time Dependent and Spatially Varying Flows*, D. L. Dwoyer and M. Y. Hussaini (eds.), pp. 43-57, Springer Verlag, New York, 1987.
- [13] Zang, T. A.; and Hussaini, M. Y.: Numerical Experiments on the Stability of Controlled Shear Flows, AIAA Paper No. 85-1698, 1985.
- [14] Zang, T. A.; and Hussaini, M. Y.: On Spectral Multigrid Methods for the Time-Dependent Navier-Stokes Equations, *Appl. Math. Comp.*, Vol. 19, 1986, pp. 359-372.
- [15] Hussaini, M. Y.; and Zang, T. A.: Spectral Methods in Fluid Dynamics, *Ann. Rev. Fluid Mech.*, Vol. 19, 1987.
- [16] Canuto, C.; Hussaini, M. Y.; Quarteroni, A.; and Zang, T. A.: *Spectral Methods in Fluid Dynamics*, Springer-Verlag, Berlin, 1987.
- [17] DiPrima, R. C.; and Swinney, H. L.: Transition in Flow between Rotating Concentric Cylinders, *Transition and Turbulence*, R.E. Meyer (ed.), Academic Press, 1981.
- [18] Benjamin, T. B.: Bifurcation Phenomena in Steady Flow of a Viscous Fluid I. Theory, *Proc. Roy. Soc. London*, Vol. A 359, 1978, pp. 1-26.
- [19] Streett, C. L.; and Hussaini, M. Y.: Finite Length Effects in Taylor-Couette Flow, ICASE Report No. 86-59, 1986.
- [20] Benjamin, T. B.; and Mullin, T.: Anomalous modes in the Taylor Experiment, *Proc. Roy. Soc. London*, Vol. A377, 1981, pp. 221-249.
- [21] Erlebacher, G.; and Hussaini, M. Y.: Incipient Transition Phenomena in Compressible Flows over a Flat Plate, ICASE Report 86-39, 1986.
- [22] Bardina, J.; Ferziger, J. H.; and Reynolds, W. C.: Improved Turbulence Models Based on Large Eddy Simulation of Homogeneous, Incompressible, Turbulent Flows, Report TF-19, Department of Mechanical Engineering, Stanford University, Palo Alto, CA, 1983.

- [23] Erlebacher, G.; Hussaini, M. Y.; Speziale, C. G.; and Zang, T. A.: Subgrid-Scale Models for Compressible Turbulence, ICASE Report, 1987.

ORR-SOMMERFELD EIGENFUNCTION

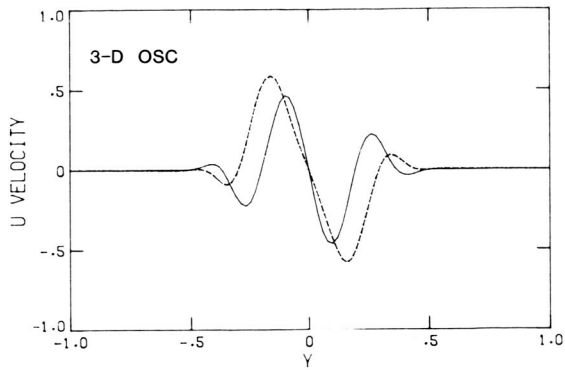


Figure 1a. Center mode.

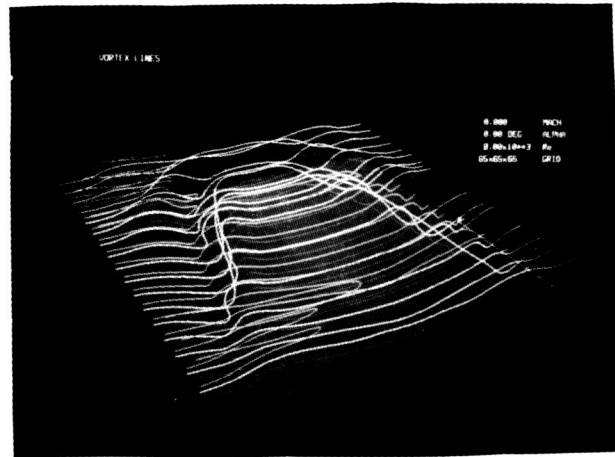


Figure 3a. Vortex lines at $t = 87$ for the center mode transition in channel flow at a Reynolds number of 8000.

ORR-SOMMERFELD EIGENFUNCTION

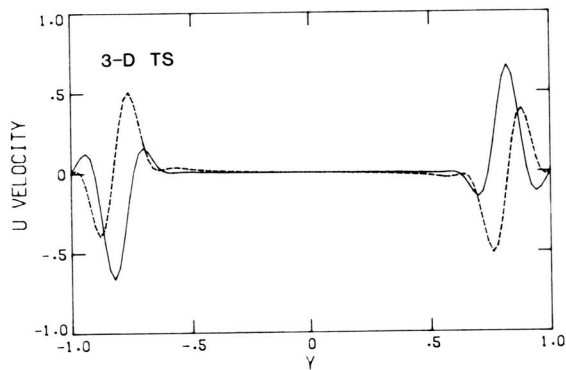


Figure 1b. Wall mode.

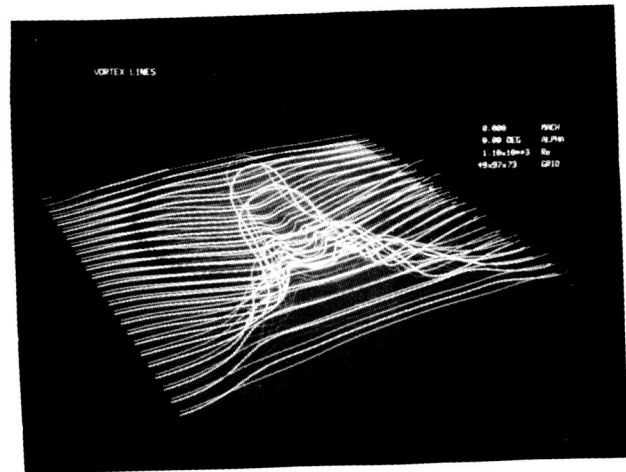


Figure 3b. Vortex lines after 3-7/8 TS periods for a (fundamental) K-type transition in a boundary layer at a Reynolds number of 1100.

10% 2-D CEN. 3.0% CEN

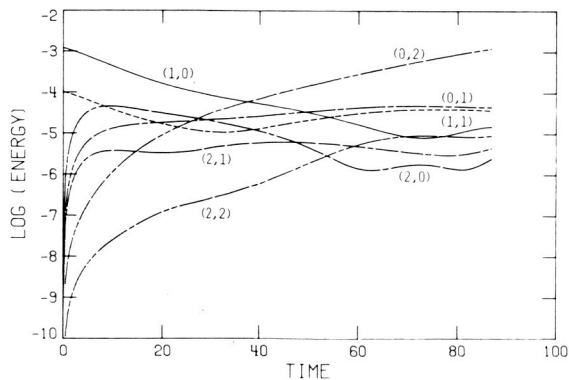


Figure 2. Harmonic history for a $Re = 8000$ center mode simulation.

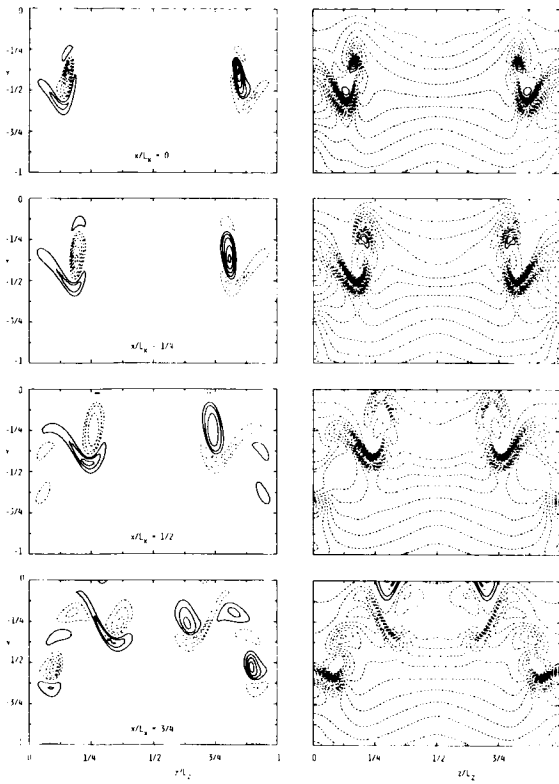


Figure 4. Streamwise (left) and spanwise (right) vorticity contours at $t = 87$ for a channel center mode at a Reynolds number of 8000. The contour interval is 0.20. Dashed lines indicate negative contours.

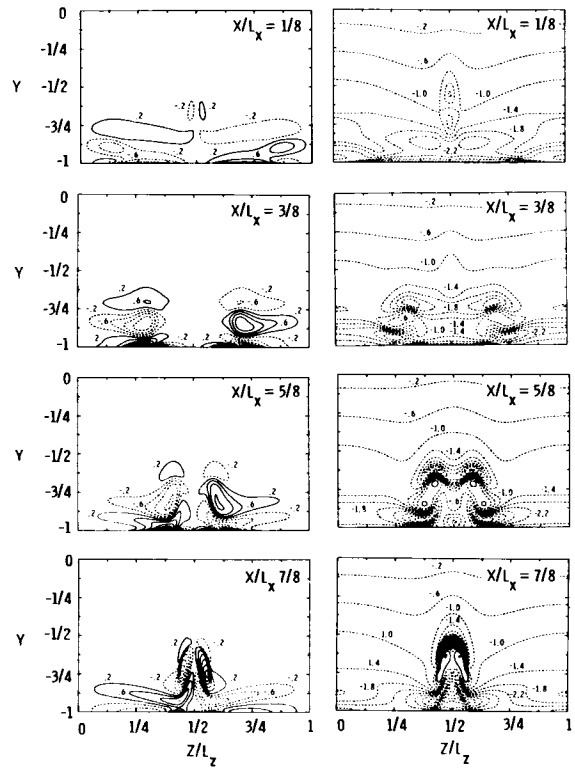


Figure 5. Streamwise (left) and spanwise (right) vorticity contours at $t = 182$ for a channel wall mode at a Reynolds number of 8000. The contour interval is 0.40. Dashed lines indicate negative contours.

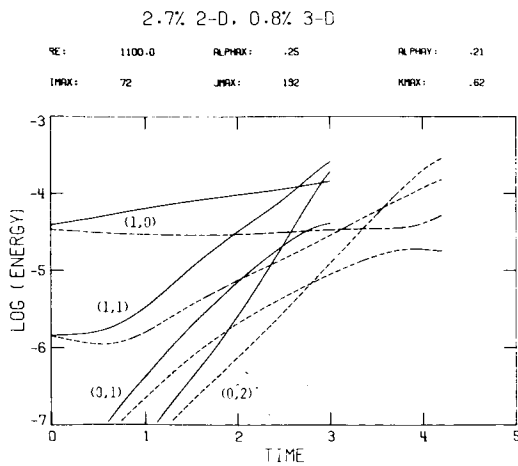


Figure 6. Harmonic energy history of an uncontrolled (solid lines) and a heated (dashed lines) boundary layer undergoing a K-type transition at a Reynolds number of 1100.

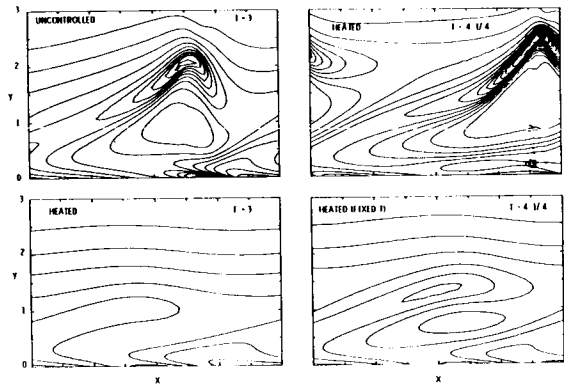


Figure 7. Vertical shear in the peak plane for $Re = 1100$ boundary layer simulation.

ORIGINAL PAGE IS
OF POOR QUALITY

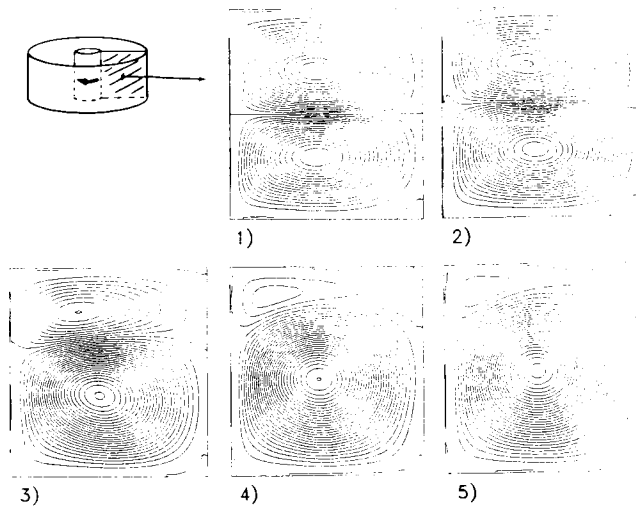


Figure 8. Cross-sectional streamline at 5 stages of two-cell/one-cell exchange process.

Harm. Cont. M=4.5 Re=10000

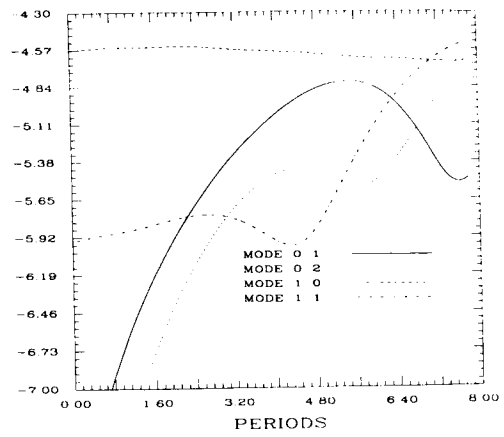


Figure 10. Harmonic energy history for a Mach 4.5 boundary layer undergoing transition at a Reynolds number of 10,000.

$$\Gamma = 1.05$$

$$\eta = .615$$

$$R = 150$$

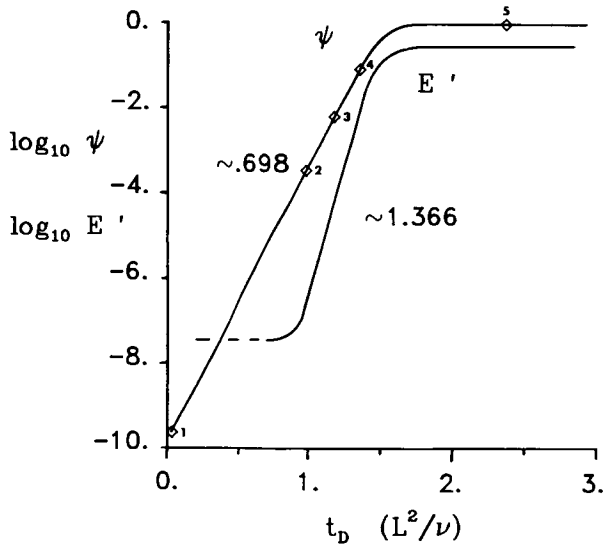


Figure 9. Time history of order parameter and perturbation energy.

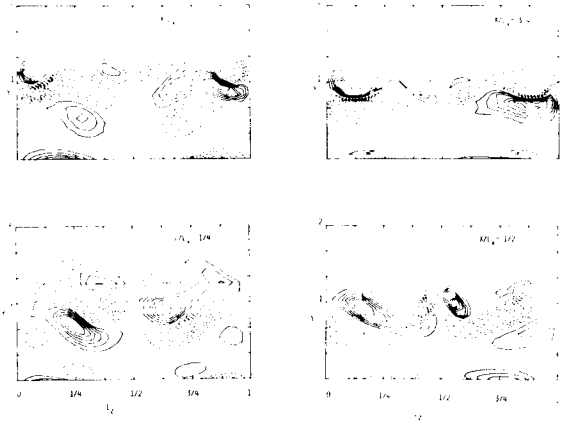


Figure 11. Streamwise vorticity contours for the compressible boundary layer transition at Mach 4.5. The contour interval is 0.20. Dashed lines indicate negative contours.

**ORIGINAL PAGE IS
OF POOR QUALITY**